



Lawrence Berkeley Laboratory

UNIVERSITY OF CALIFORNIA

Materials & Molecular Research Division

RECEIVED
LAWRENCE
BERKELEY LABORATORY

MAY 30 1980

Submitted to the Journal of Applied Physics

LIBRARY AND
DOCUMENTS SECT

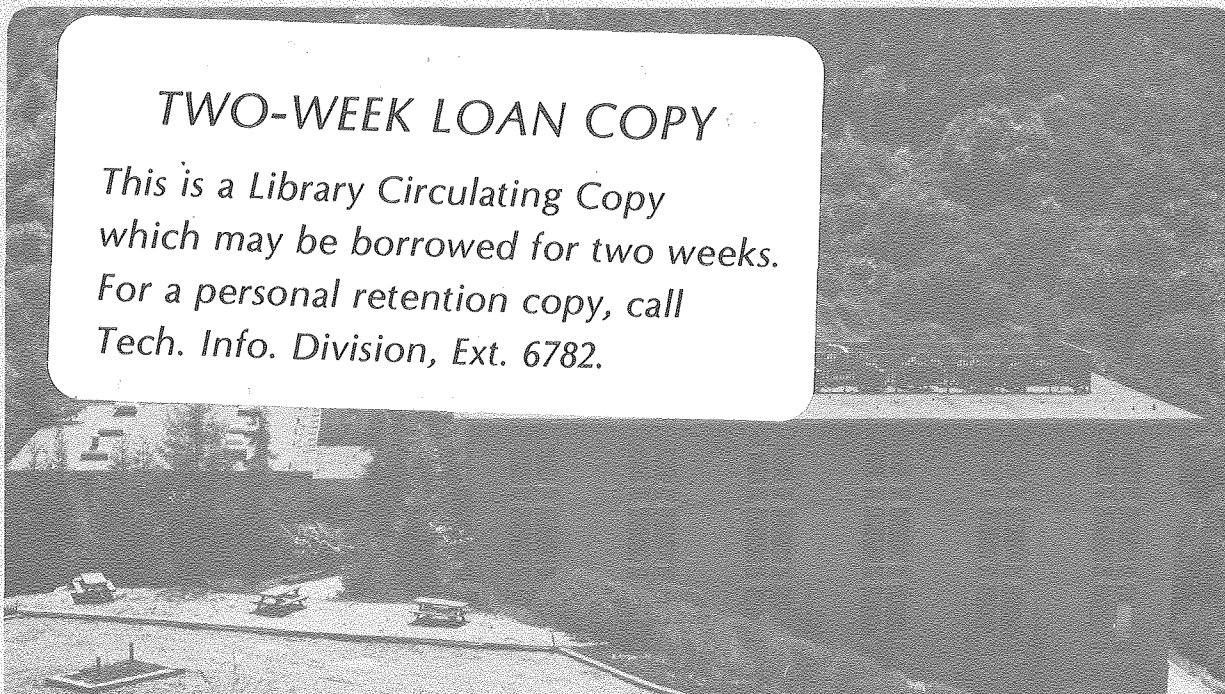
TRANSMISSION ELECTRON MICROSCOPY AND RUTHERFORD
BACKSCATTERING STUDIES OF DIFFERENT DAMAGE STRUCTURES
IN P⁺ IMPLANTED Si

D. K. Sadana, M. Strathman, J. Washburn, and G. R. Booker

March 1980

TWO-WEEK LOAN COPY

*This is a Library Circulating Copy
which may be borrowed for two weeks.
For a personal retention copy, call
Tech. Info. Division, Ext. 6782.*



LBL-10725 C-2

DISCLAIMER

This document was prepared as an account of work sponsored by the United States Government. While this document is believed to contain correct information, neither the United States Government nor any agency thereof, nor the Regents of the University of California, nor any of their employees, makes any warranty, express or implied, or assumes any legal responsibility for the accuracy, completeness, or usefulness of any information, apparatus, product, or process disclosed, or represents that its use would not infringe privately owned rights. Reference herein to any specific commercial product, process, or service by its trade name, trademark, manufacturer, or otherwise, does not necessarily constitute or imply its endorsement, recommendation, or favoring by the United States Government or any agency thereof, or the Regents of the University of California. The views and opinions of authors expressed herein do not necessarily state or reflect those of the United States Government or any agency thereof or the Regents of the University of California.

TRANSMISSION ELECTRON MICROSCOPY AND RUTHERFORD BACKSCATTERING
STUDIES OF DIFFERENT DAMAGE STRUCTURES IN P⁺ IMPLANTED Si

D.K. Sadana, M. Strathman, J. Washburn
Lawrence Berkeley Laboratory
University of California, Berkeley, CA 94720

G.R. Booker
Department of Metallurgy
University of Oxford, Oxford OX1 3PH (England)

ABSTRACT

'Cross-sectional transmission electron microscopy (TEM)' and MeV He⁺ channelling methods have been used to examine different damage structures present under the colour bands visible at the surface of a high dose rate P⁺ implanted (111) Si implanted to a dose of 7.5×10^{15} ions/cm². TEM and channelling results obtained from individual coloured regions showed a good qualitative correlation in that discrete damage layers observed in the 'cross-sectional TEM' micrographs appeared as discrete peaks in the channelled spectra. The mean depths of the damage layers obtained from these two methods were in agreement. However, the widths of the deeper lying damage layers calculated from the channelling measurements were always greater than the widths observed by TEM. An empirical method based on subtraction of dechannelling background in the channelling spectra gave damage layer widths that were in close agreement with the TEM results.

INTRODUCTION

The present study is concerned with the comparison of transmission electron microscopy (TEM) and channelled Rutherford backscattering (RBS) methods to examine different damage structures occurring in ion-implanted Si. For this purpose, a high dose rate P^+ implanted Si wafer was chosen. It has been observed by earlier workers¹⁻⁴ that if the thermal contact of the wafer being implanted under high dose rate conditions is not good, it gives rise to varying damage structures across the implanted wafer due to non-uniform heating during the implantation. This results in the appearance of bands of different color at the implanted surface due to optical interference effects between light reflected from the surface and from the variable depth of the sub-surface interface at which the refractive index changes occur.^{2,4} These specimens were convenient for the present experiments because they provided several types of secondary damage layers in the same specimen. A model for the appearance of bands of different colors at the surface of such specimens has been reported elsewhere.⁴

In the present experiment, TEM 90° cross-section specimens were prepared from different colored regions in the multi-colored band (this region represents different implantation-temperatures) to obtain 'visible damage'-depth distributions for each color band. The nature of the damage present in the individual bands was further revealed by 'plan view' specimens. The nature and damage distribution beneath each particular color band was found to be entirely different from that present beneath the adjacent color band.

Channelled RBS measurements were also taken from each individual color band and the results were compared with the TEM results. A good

quantitative correlation between the results obtained from these two techniques was observed by the use of an empirical method to analyze the channelled RBS results.

EXPERIMENTAL

a. Implantation

P-type, 17 ohm cm, (111) Si slices of 5 cm diameter were implanted in a non-channelling direction with 120 KeV P^+ ions to a dose of $7.5 \times 10^{15}/\text{cm}^2$. The implantation energy of 120 KeV corresponded to an LSS projected range of 1500Å with straggling of $\pm 530\text{Å}$.⁵ The implantation was carried out in the MRIV Harwell-Linnett isotope separator. The wafers were scanned through 3 cm long line focus ion beam by double axis mechanical scanning. The details of the implantation chamber are described elsewhere.⁶ The implantation time was fixed to 10 minutes. The maximum implantation temperature is estimated to have increased up to 400°C by the end of the scanning cycle.

b. TEM

For TEM studies, both '90° cross-section' and 'plan' view specimens were prepared. The former specimens were obtained by cleaving the slices from different colored regions in the multi-colored band and then mechanically polishing followed by low energy ion-beam thinning, as described previously.⁷ The 'cross-section' micrographs obtained correspond to the (110) plane perpendicular to the original (111) specimen surface plane. The 'plan view' specimens were prepared by chemical jet thinning the specimens from the unimplanted side using a HF:HNO₃ solution. All the TEM examinations for the 'cross-sectional' specimens were performed using the bright field, strong beam diffraction contrast method. The specimens were tilted to two beam conditions for a

220 type reflection. Transmission electron diffraction patterns (TEDs) were obtained to aid in the identification of the damage, using the standard selected area method.

c. RBS/Channelling

1.7 MeV He^+ beam was accelerated in a Van de Graff generator with an energy resolution of ± 500 eV. The beam was momentum analyzed by 25° to filter the undesired elements present in it and was then collimated to approximately 1 mm diameter spot size using successive sets of tantalum and stainless steel collimators. A Si surface barrier detector with a resolution of 14 KV FWHM for (1-6) Mev particles was mounted approximately 14 cms away from the target. The backscattered particles were detected by the detector at an angle of 170° with respect to the beam. The output was stored in a Tracer Northern 512/1024 MCA. For current integration, a magnetic Faraday Cup arrangement was used. The details of the magnetic Faraday cup set-up are given elsewhere.⁸ The widths of the color bands varied from approximately 0.5 mm to 2 mm. Therefore, for the channelled spectra, only the bands wider than the beam diameter were examined. A schematic diagram showing the color sequence of the bands is shown in Fig. 1.

In order to channel the beam into the crystal and position it at different parts of the crystal very precisely, a special specimen stage with five degrees of freedom; viz., two independent tilts, ϕ and θ , and independent 360° rotation with respect to the beam, each with a precision of $\pm 0.05^\circ$ and independent x and y translational movements, each with a precision of ± 0.01 cm was fabricated.

The mean depths of the damaged regions were calculated by taking the energy difference of the surface peak and the damage peak in question. The energy difference was then converted into the depth scale using the energy loss tables given in Ref. 9. The widths of the damaged region was calculated taking half width of half maximum and multiplying by 2 (see Fig. 6) and were obtained from as recorded curves.

RESULTS

TEM: For the specimen chosen from the part of Si wafer that remained unheated during the implantation (marked as 'cold' in Fig. 2), the 'cross-section' micrographs showed a uniform featureless damage layer 'A' (Fig. 2a) continuous from the surface. TED pattern (micrographs not included in the text) taken from the 'plan-view' specimen for the region with thickness less than that of band 'A' (Fig. 2a), showed characteristic diffuse rings, indicating that the material in band A was amorphous. The pattern from the thicker region, that included the material in band A and a part of the underlying substrate consisted of diffuse rings together with single crystal spots.

For the specimens showing the green band at the implanted surface, TEM 'cross-section' micrographs (Fig. 3a) showed two discrete buried damage layers, D_1 and D_2 . The regions F_1 and F_2 above and below the layer D_1 were free of 'visible damage' (data, Table I). The term 'visible damage' refers to the damage visible by TEM. TED pattern (micrographs not included in the text) from the 'plan-view' specimens corresponding to region F_1 in Fig. 3a consisted of faint diffuse rings together with single crystal spots indicating that the surface region was heavily damaged and there were amorphous zones imbedded in the crystalline matrix; however, the patterns from the thicker region that

included regions F_1 , D_1 , F_2 , D_2 and a part of the substrate material consisted of well defined and more intense diffuse rings indicating that the damage in the layers D_1 and D_2 had more percentage of an amorphous material than in the region F_1 .

For the specimens showing a violet band at the implanted surface, TEM 'cross-section' micrographs (Fig. 4a) again showed two discrete buried damage layers L_1 and L_2 ; however, the damage widths sequence was now in the reverse order as compared to that in the green band specimen. The first damage layer L_1 was narrow and consisted of damage clusters and coarse damage, but the second and deeper lying layer L_2 was wider and had a dense structure within it (data, Table I). The regions T_1 and T_2 above and below the layer L_1 were free of 'visible damage.' TED patterns (not included in the text) taken from 'plan view' specimen gave similar results to that obtained for the green band specimen.

For the specimen that experienced the maximum heating during the implantation (marked 'clear' in Fig. 1), 'cross-section' micrographs (Fig. 5b) showed a buried damage layer 'N' consisting of small damage clusters (data, Table I). The regions U_1 and U_2 above and below layer N were free of 'visible damage.' TED pattern (micrographs not included in the text) taken from 'plan view' specimen corresponding to region U_1 consisted of single crystal spot patterns, indicating that the material in this region was single crystal. The imbedded amorphous regions near the surface, as indicated by TED patterns for the previous three specimens were no longer present. The pattern remained practically unchanged on going from region U_1 to the region that included band N and part of the substrate material, indicating that the damage in the band N was single crystalline in nature.

RBS/channelling

The depth profiles of the damage described in this section were obtained from the channelled spectra using the surface energy approximation method.⁹ The channelled and random spectra for virgin single crystal, shown by the broken lines in Fig. 2b-5b are also included with the spectra obtained from the various colored regions of the implanted specimen in order to interpret the extent of disorder present in the damaged regions under an individual color band.

The channelled spectra obtained from the color band regions are described as follows:

For the region of Si wafer that remained unheated during the implantation and is marked as 'cold' in Fig. 1, the channelled spectrum showed only one peak with a 'flat top'(Fig. 2b). The surface peak 'S' present in the channelled spectrum for the 'virgin' crystal was absent in the spectrum for the 'cold' region. The scattering yield for the 'flat-top' was the same as that for the random spectrum, indicating that the disordered region was either amorphous or randomly oriented. The calculated mean depth and width of the damaged region is given in Table I.

For the region showing the green band at the implanted surface, the channelled spectrum showed three distinct peaks: G_1 , G_2 , and G_3 (Fig. 3b). The peak G_1 at energy 0.96 MeV corresponded to the surface peak 'S' in the channelled spectrum for the 'virgin' crystal, indicating that the surface region was single crystal in nature. However, the increase in the peak height (scattering yield) as compared to that of 'virgin' crystal indicated that the surface region was heavily damaged. The peaks G_2 and G_3 at energies 0.9 MeV and 0.86 MeV, respectively, showed that two distinct damage regions separated by a relatively less

damaged region were present under the damaged surface region. The magnitude of the scattering yield values for these peaks indicated that the damage in the first layer was very dense and close to amorphous in nature, but the second damage layer was less dense. The mean depths and widths of the damage layers calculated from the spectra are given in Table I.

For the specimen showing a violet band at the implanted surface, the channelled spectrum again showed three distinct damage peaks: B_1 , B_2 and B_3 (Fig. 4b). The peak B_1 at energy 0.95 MeV again corresponded to the surface peak 'S' in the channelled spectrum for the 'virgin' crystal indicating that the surface region was single crystal in nature. However, the height of peak B_1 was less than that of peak G_1 (Fig. 3b) but was greater as compared to peak S indicating that although the surface region was still damaged, the amount of disorder was less than that present in the surface region of the green band specimen. The peaks B_2 (0.9 MeV) and B_3 (0.85 MeV) indicated that there were two distinct damage layers separated by a relatively less damaged region. However, the first damage layer was much narrower as compared to the second. The scattering yield values showed that in contrast to the results observed for the green band specimen, the first narrow damage layer has less disorder as compared to the second wide damage layer. Table I gives the mean depths and widths for these damage layers.

For the region that appeared to be 'clear' and corresponded to the region that experienced the maximum heating during the implantation, the channelled spectrum showed only two peaks M_1 and M_2 (Fig. 5b). The height and energy value of the first peak M_1 was the same as that obtained for the violet band region. These results indicated that the amount of disorder near the surface progressively decreased as the implantation temperature increased due to beam heating effect. The

disorder attained a constant value at the end of the implantation cycle. The second peak M_2 at an energy of 0.87 MeV showed the presence of a buried layer of damage. The scattering yield value indicated that the amount of disorder present within this damage layer was significantly less than that observed in the main damage layers of the green or blue band. The mean depth and width of the damage layer N is included in Table I.

DISCUSSION

The results of the damage layers as obtained by TEM and channelled RBS method are listed in Table 1. It is clear from Figs. 2-5 that there is a good qualitative correlation between the results obtained by the two methods. The discrete damage layers as seen by TEM appeared as the discrete damage peaks in the channelled RBS spectra. The extent of disorder as revealed by TEM cross-section micrographs and indicated by TED patterns also correlated very well with the scattering yield values obtained by the channelled spectra. For example, the TEM results showed that the first damage layer D_1 under the green band consisted of more disorder as compared to that in the first damage layer L_1 under the violet band and vice versa for the second damage layer. The scattering yield values from the channelled spectra also followed precisely the same pattern. However, further comparison of the TEM and channelled RBS data for the damage layers as given in Table 1 showed that, although the mean depths of the damage layers obtained from the two methods were in close agreement, the widths of the damage layers as calculated from the channelled RBS method consistently gave higher values.

Energy straggling in the back scattered beam due to the damage was first thought to be responsible for the discrepancy in the results.

Therefore, the contribution due to energy straggling was incorporated in the calculations previously done using the surface approximation method.⁹ An energy straggling contribution was assigned at a particular depth based on the data of Harris and Nicolet.¹⁰ Although this resulted in an improvement in the correlation of the the data, there still was a considerable disagreement. The damage layer widths obtained after applying energy straggling correction are also given in Table 1.

It was observed that the dechannelling of the beam due to the interaction with the disorder nearer the surface gave a "background" at lower energies that was superimposed on the spectra due to the deeper damage. The dechannelling due to the surface damage had a "background" on the lower energy side which was frequently approximately equal to half the amplitude of the surface peak in this experiment. Several spectra containing single buried damage bands were also found to have "backgrounds" on the low energy side of the peak of the order of half the value of the peak height. Therefore, the "background" level due to each scattering peak was assumed to be independent of that from the others and to have a magnitude of half the height of the peak for all lower energies. Therefore, for peaks, due to buried layers of damage, the half width at half maximum was taken at a scattering yield half way between the background resulting from all the higher energy peaks and the top of the peak in question. Figure 7 shows a schematic representation of the "background" subtraction method used here. The layer widths calculated this way were in close agreement with the TEM results (Table 1). The layer widths were also calculated by approximating the 'background' as a smooth curve passing underneath the minima in the spectra until the curve approached the low energy region deep inside the crystal where there was no damage (Fig. 6).⁹ The layer widths obtained this way were also in

good agreement with the TEM results. However, the uncertainty was considerable for the cases such as Figs. 3 and 4 where the minima in the channelling spectra were not distributed in a manner as shown in Fig. 6. The 'smooth background curve' could then be drawn in several different ways. Although both empirical methods gave complementary results, the subjective scatter in calculations was found to be much less by using the empirical method described in the present paper.

The "background" subtraction method described above for a single damage band was also applied to the multi-damage band case. Here a "background" of half the peak height was assigned to each peak, starting from the surface and iterating into the crystal.

Conclusions The following conclusions can be drawn from the present study:

1. The discrete damage layers seen in the TEM cross-section micrograph appear as discrete damage peaks in the channelled RBS spectra.
2. The damage layers widths as obtained from the channelled RBS spectra using the ordinary surface approximation method consistently gives higher values as compared to the values obtained from TEM cross-section micrographs.
3. An empirical method based on subtraction of the dechannelling background gives damage layer widths that are in close agreement with the TEM results.

ACKNOWLEDGEMENTS

The authors would like to thank Jim Hodges and Steve Klingeler who designed and fabricated the specimen stage for the channelling measurements; Scott Hubbard and Dan Meier for their help in improving the performance of the equipment at various stages of the work and Jim Stephens and D. Chivers of AERE Harewell (England) for implanting the Si wafers. The authors are grateful to Marc-A. Nicolet, Jim Mayer and I. Golecki of the California Institute of Technology and to George Gabor of this Laboratory for the useful discussions and comments on the paper. Finally, we would like to acknowledge the financial support of the Department of Energy through the Material and Molecular Research Division and the Department of Instrument Techniques of Lawrence Berkeley Laboratory.

REFERENCES

1. J.H. Freeman, D.J. Chivers, G.A. Gard, G.W. Hinder, B.J. Smith and J. Stephen, Ion Implantation in Semiconductors, Ed. S. Namba (Plenum Press: New York, 1975). pp 555-569.
2. L. Csepregi, E.F. Kennedy, S.S. Lau, J.W. Mayer and T.W. Sigmon, App. Phys. Lett., 29, 645 (1976).
3. T.E. Seidel, G.A. Pasteur and J.C. Tsai, App. Phys. Lett., 29, 648 (1976).
4. D.G. Beanland, Rad. Eff., 33, 219 (1977).
5. J.F. Gibbons, W.S. Johnston and S.W. Myglorie, Projected Range Statistics, Semiconductors and Related Material, John Wiley and Sons (1975).
6. J.H. Freeman, L.R. Caldecourt, K.C.W. Done and J. Francis, Proc, Conf. on Ion Implantation, Reading (Peter Peregrinus, Stevenage) 1970 and AERE Report R 6496 (1970).
7. H.R. Pettit and G.R. Booker, IOP London Conf Series, 10, 290 (1971).
8. M. Strathman and M. Green (unpublished).
9. W.K. Chu, J.W. Mayer and M-A Nicolet, Backscattering Spectrometry (Academic Press, 1978), Chapt. 4, pp. 89-122.
10. J.M. Harris and M-A. Nicolet, Phys. Rev., 11, 1013 (1975).

FIGURE CAPTIONS

Fig. 1. $P^+_{\rightarrow}(111)$ Si, $7.5 \times 10^{15}/\text{cm}^2$, 120 KeV. A schematic diagram showing color sequence at the implanted surface.

Fig. 2. Comparison of cross-sectional TEM and channelling spectrum for the 'cold' specimen.

Fig. 3. Comparison of cross-sectional TEM and channelling spectrum for the 'green band' specimen.

Fig. 4. Comparison of cross-sectional TEM and channelling spectrum for the 'violet band' specimen.

Fig. 5. Comparison of cross-sectional TEM and channelling for the 'hot' specimen.

Fig. 6. A schematic representation of the empirical method used to subtract the dechanelling 'background.'

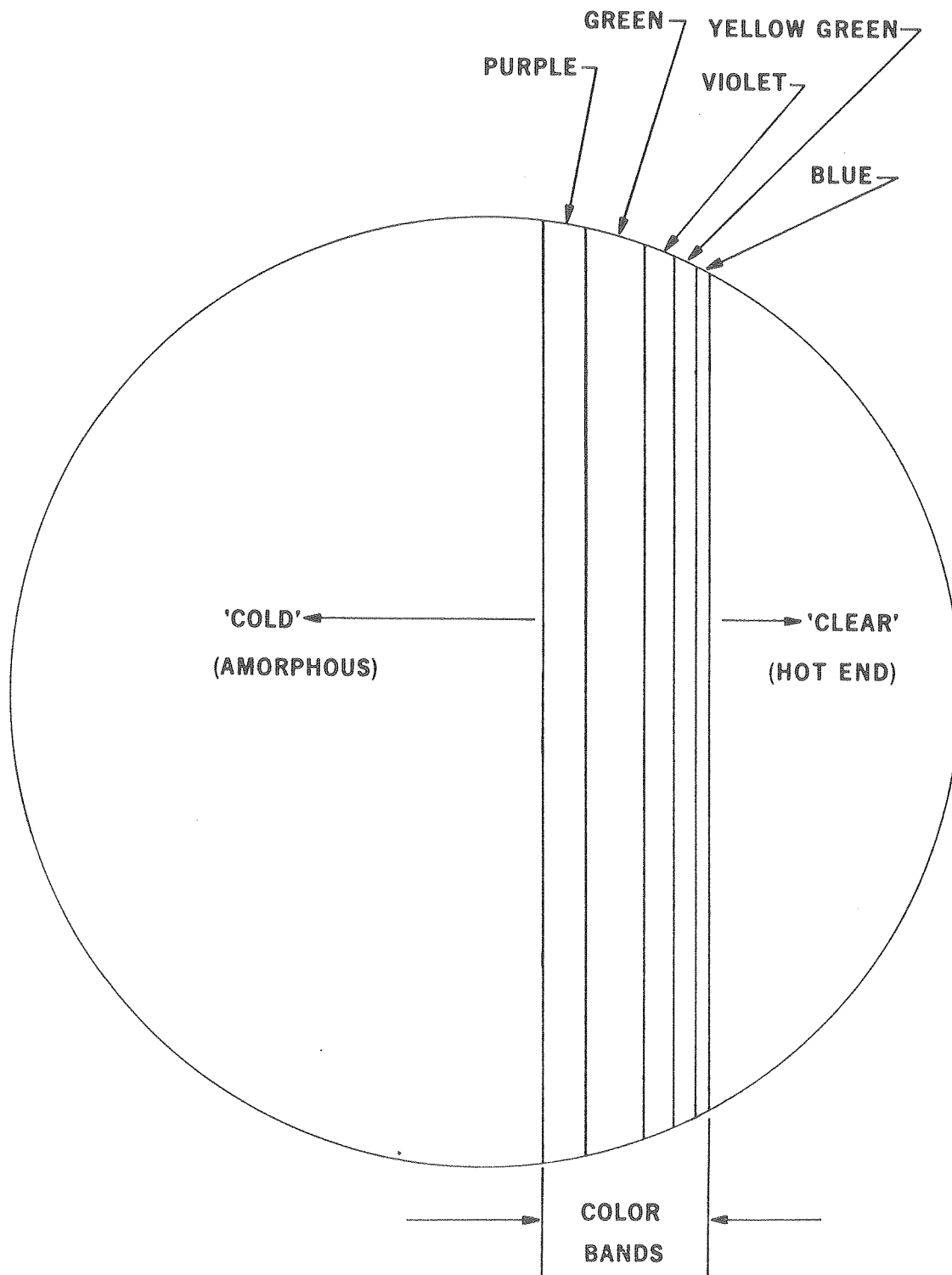
Table I

Color of the Band	TEM				CHANNELLING			
	Upper Damage Layer		Lower Damage Layer		Upper Damage Layer		Lower Damage Layer	
	Mean Depth(Å)	Width (Å)	Mean Depth(Å)	Width (Å)	Mean Depth(Å)	Width (Å)	Mean Depth(Å)	Width (Å)
'Cold'	980	1960	---	---	1050	2400 ^a , 2370 ^b 2020 ^c	---	---
Green	800	870	1560	550	800	920 ^a , 900 ^b <u>850^c</u>	1600	1040 ^a , 1010 ^b , <u>500^c</u>
Violet	800	340	1500	870	800	960 ^a , 940 ^b <u>350^c</u>	1470	1520 ^a , 1490 ^b <u>850^c</u>
'Clear'	1270	930			1300	1750 ^a , 1720 ^b <u>900^c</u>		

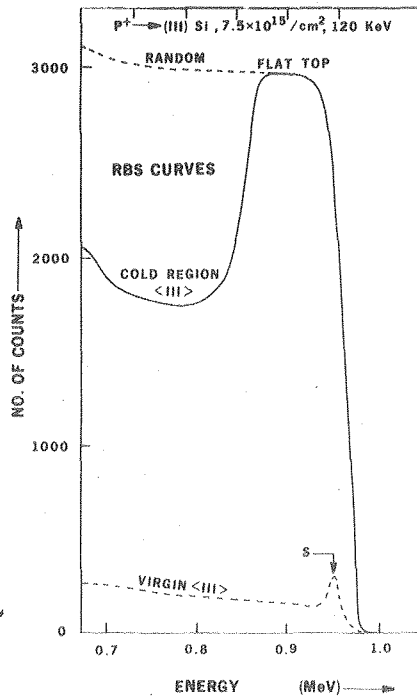
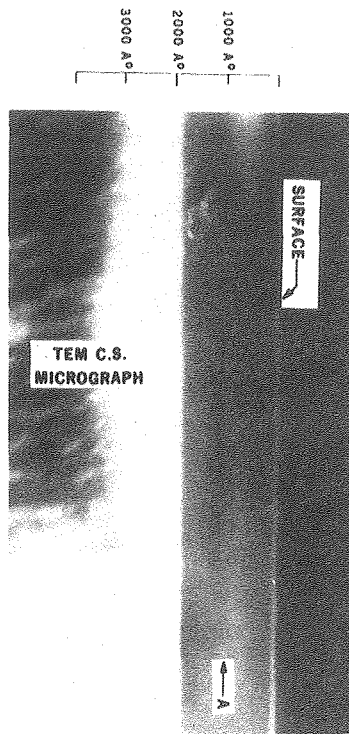
a. Using surface approximation only.

b. Using surface approximation with energy straggling factor incorporated.

c. Using surface approximation and subtracting the "background" (our empirical method). These values were found to differ by +5% due to human error.



(17)



XBB 790-13568

